

Electronic supplementary information

## Highly Conductive, Pliable and Foldable Cu/Cellulose Paper electrode Enabled by Controlled Deposition of Copper Nanoparticles

Yang Yang,<sup>a</sup> Quanbo Huang,<sup>a</sup> Gregory F. Payne,<sup>b</sup> Runcang Sun,<sup>c</sup> and Xiaohui Wang\*<sup>a</sup>

<sup>a</sup>State Key Laboratory of Pulp and Paper Engineering, South China University of Technology, Guangzhou 510640, China

<sup>b</sup>Fischell Department of Bioengineering and Institute for Bioscience and Biotechnology, University of Maryland, College Park, Maryland, MD 20742, USA

<sup>c</sup>Liaoning Province Key Laboratory of Pulp and Papermaking Engineering, Dalian Polytechnic University, Dalian, Dalian 116034, China

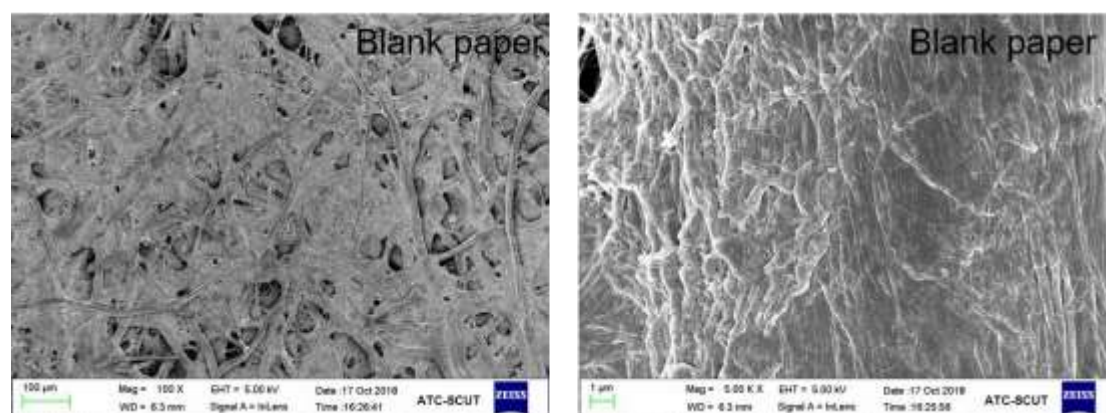


**Fig. S1** FESEM images of blank paper. It can be seen that the cellulose fibers have a smooth surface and they contain a lot of microfibril.

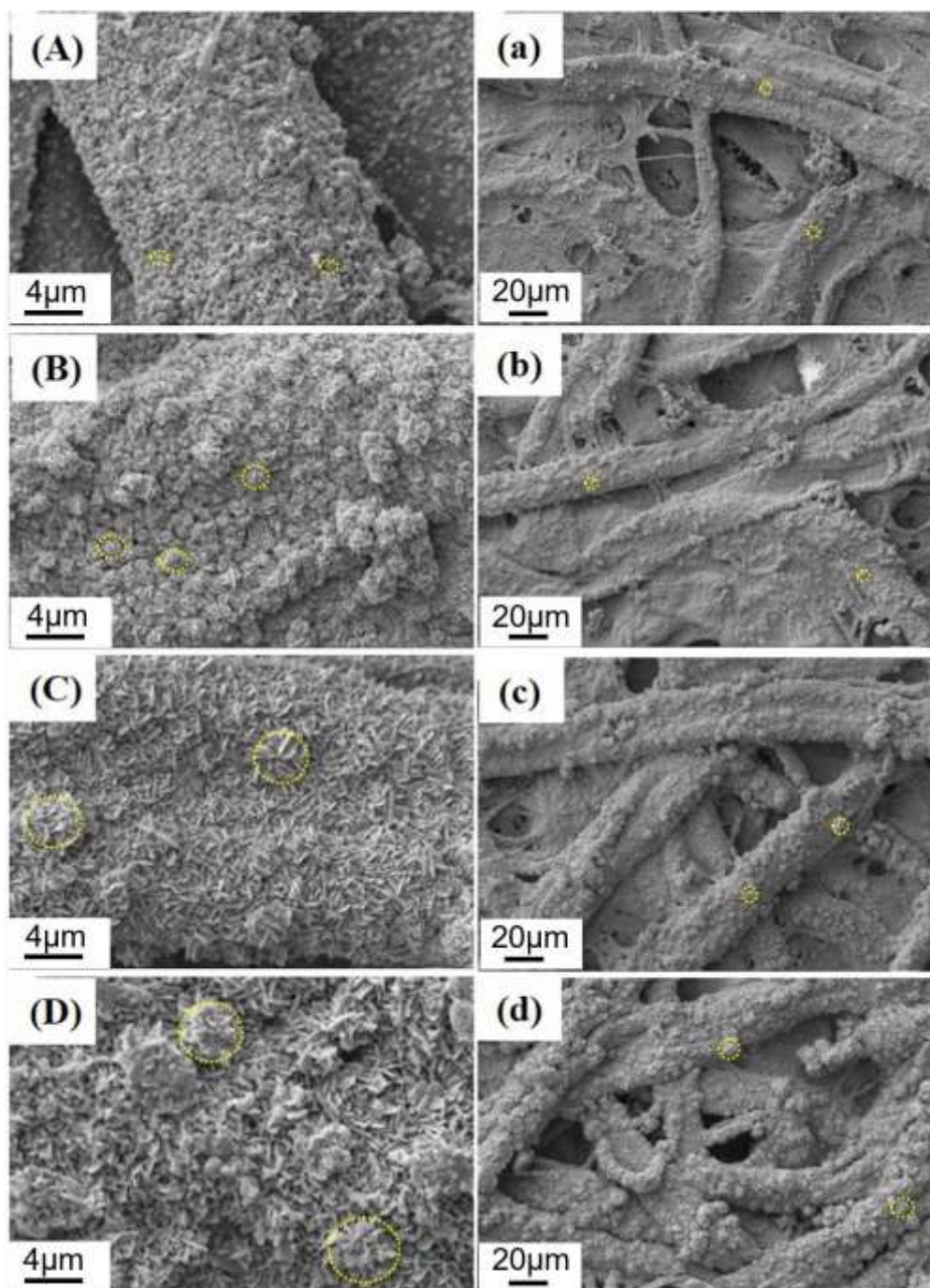


**Fig. S2** SEM images of Cu/cellulose papers with different ELD time. (A-D) SEM images of the Cu NPs coated filter paper with ELD time of 5, 10, 20, 30 min. (A-D) were partially enlarged images of a-d) The yellow circles mean the microstructure of papillae, whose size were increased with the increased ELD time.

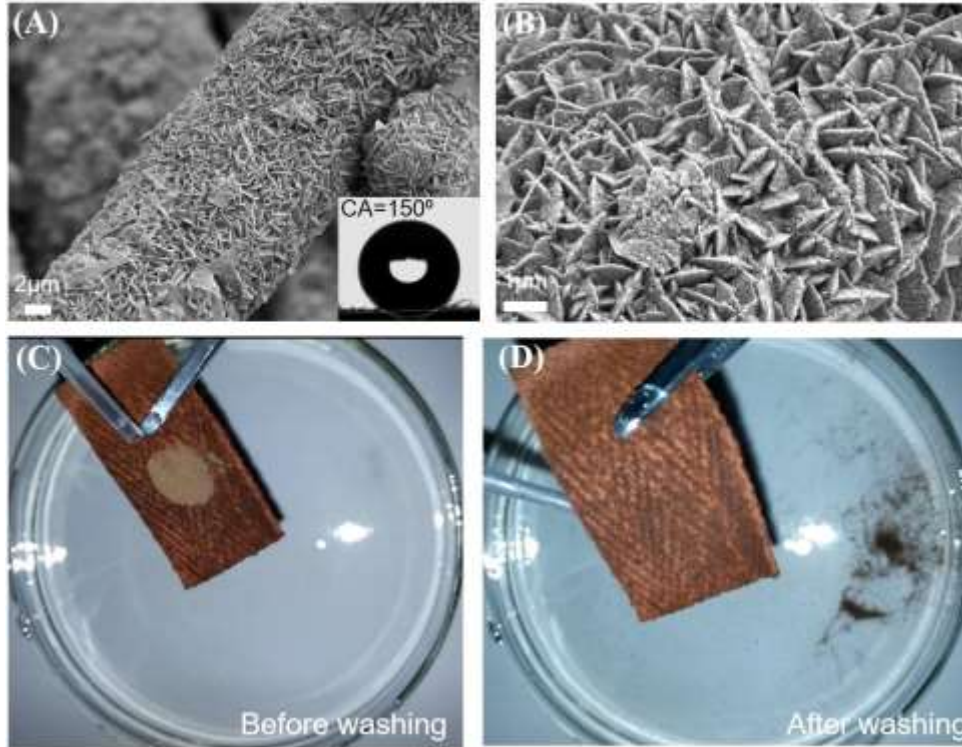


**Fig. S3** The binary nanostructure and self-cleaning property of fabrics. (A-B) FE-SEM images of Cu coated fabric. The inserts show the water contact angle measurement. (C-D) Images of dirty contaminated fabrics before and after washing.

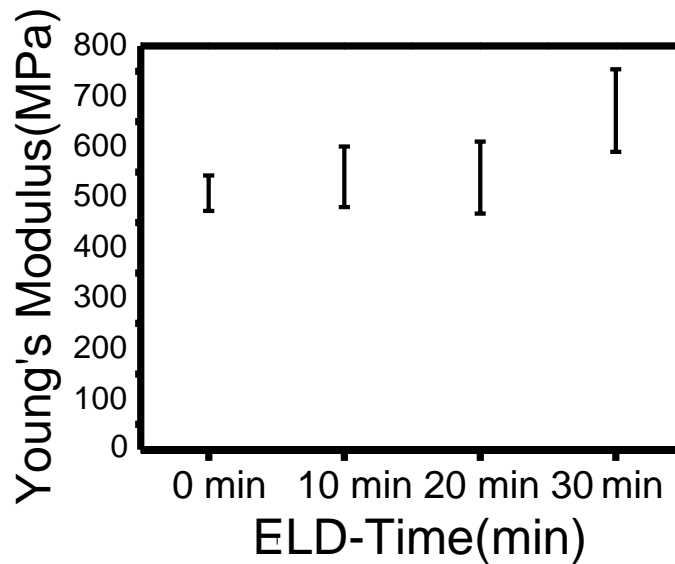


**Fig. S4** Young's Modulus for blank paper and Cu papers with different ELD time.

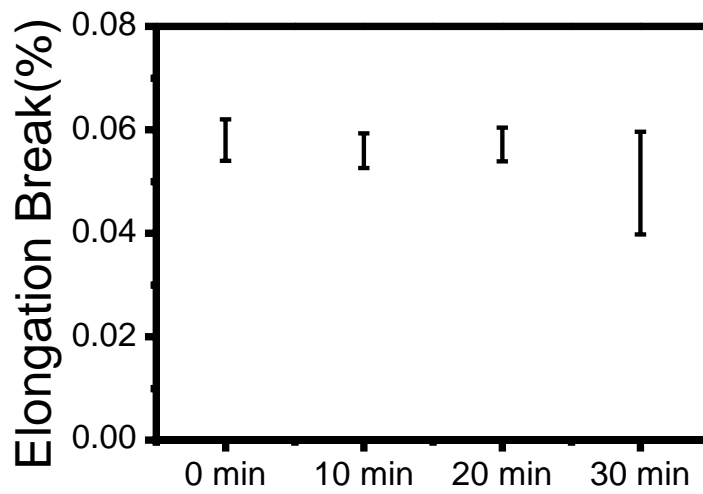


**Fig. S5** The elongation to break of Cu/cellulose papers with different ELD time.

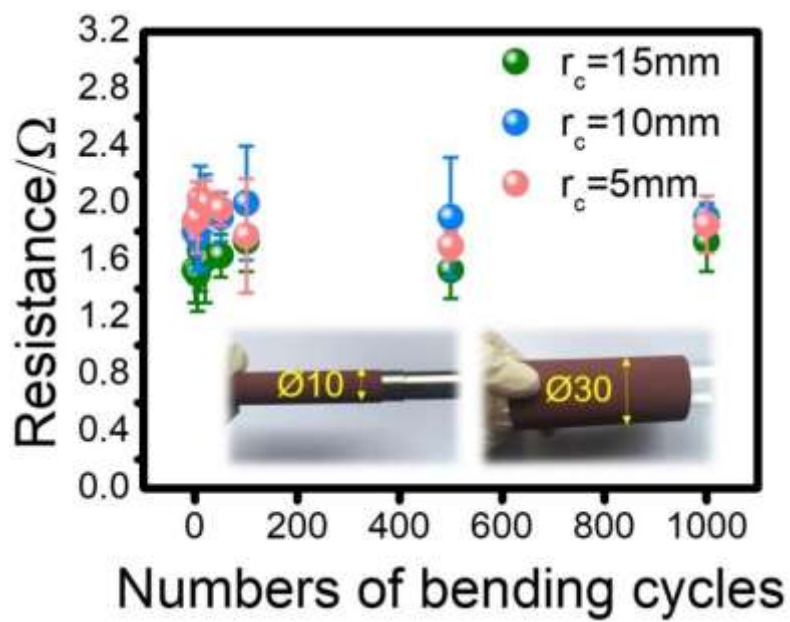


**Fig. S6** Resistance changes of the Cu/cellulose paper for different bending radius of curvature.

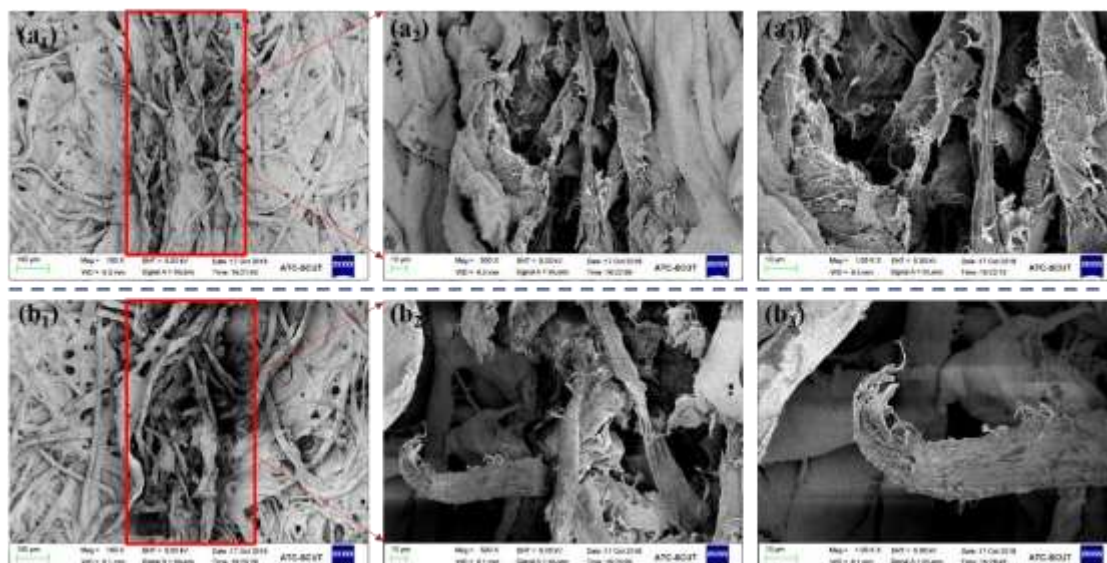


**Fig. S7** FESEM images of Cu/cellulose paper with folding time of 10(a) and 50(b). It can be seen that the cellulose fibers were becoming loose and even fibrillated or broken with increasing folding time, which blocked the transfer of electrons.

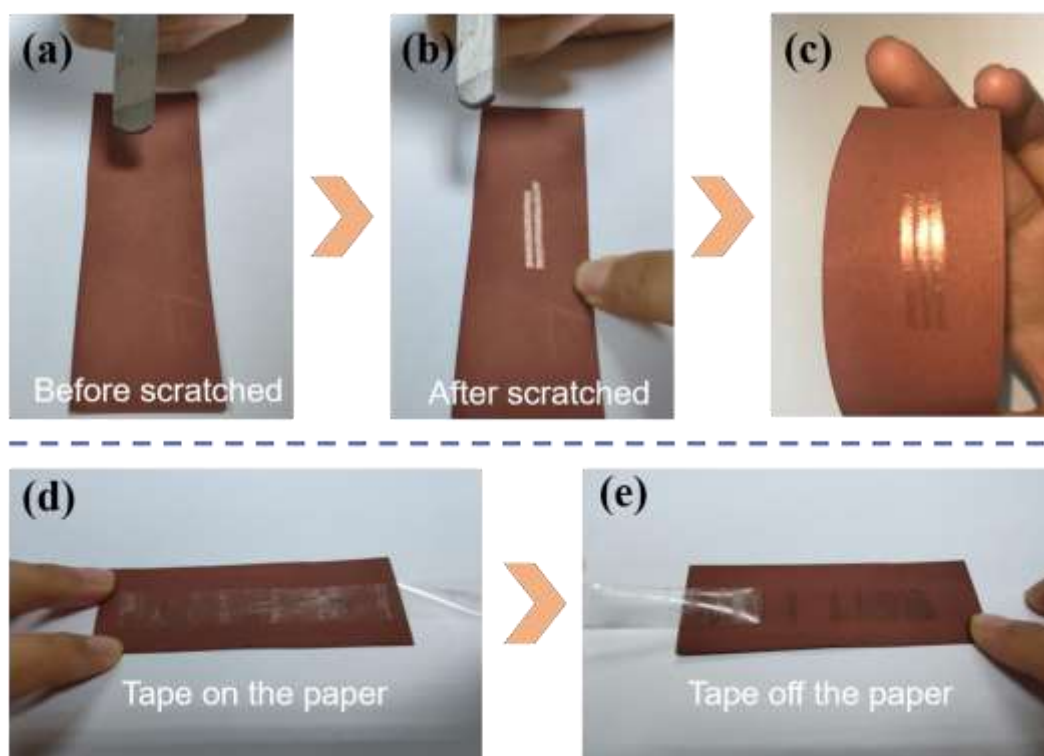


**Fig. S8** Stability performance of Cu/cellulose paper. (a-c) Cu/cellulose paper was scratched by a piece of steel. (d-e) Tape adhesion test of Cu/cellulose paper.

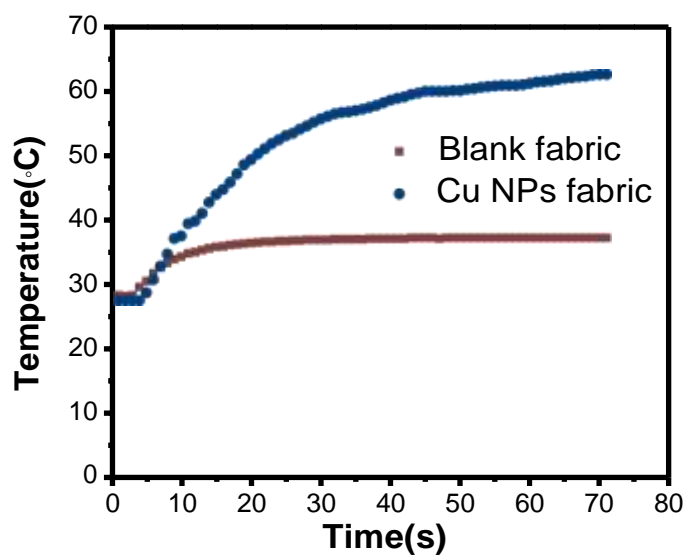


**Fig. S9** Temperature profiles of blank fabric and Cu/cellulose fabric.

## **Electrical sensing of glucose using flexible Cu/cellulose paper sensor**

**Methods for glucose sensing:** Cyclic voltammetric (CV) and amperometric (i-t) measurements were operated by using CHI 660D working station (Shanghai Chenhua Instruments Co.). The reference and the counter electrodes adopted in tests are Ag/AgCl electrode and Pt wire, respectively. The electrolyte used is NaOH solution. Before amperometric detection of glucose, we optimized possible experimental parameters that may affect the analytical performance of the fabricated nonenzymatic sensor involving concentrations of glucose and NaOH, scan rate, applied potential. More specifically, 1) For glucose concentration, the cyclic voltammograms (CVs) of the Cu/cellulose paper electrode in the presence and absence of 2 mM glucose were conducted in 100 mM NaOH solution at a scan rate of 100 mV s<sup>-1</sup>. CVs of the conductive paper in the presence of glucose with different concentrations were conducted in 100 mM NaOH, the scan rate is 100 mV s<sup>-1</sup>. 2). For NaOH concentration, CVs of the conductive paper with the appearance of 2 mM glucose under different concentrations of NaOH were conducted, while the scan rate is 10 mV s<sup>-1</sup>. 3). For scan rates, CVs of conductive paper at scan rates varying from 5 to 300 mV s<sup>-1</sup> in 100 mM NaOH solution containing 2 mM glucose were conducted. 4). For potential, real time current response of conductive paper at various potentials in the range of 0.4-0.7 V with successive additions of 2 mM glucose was conducted.

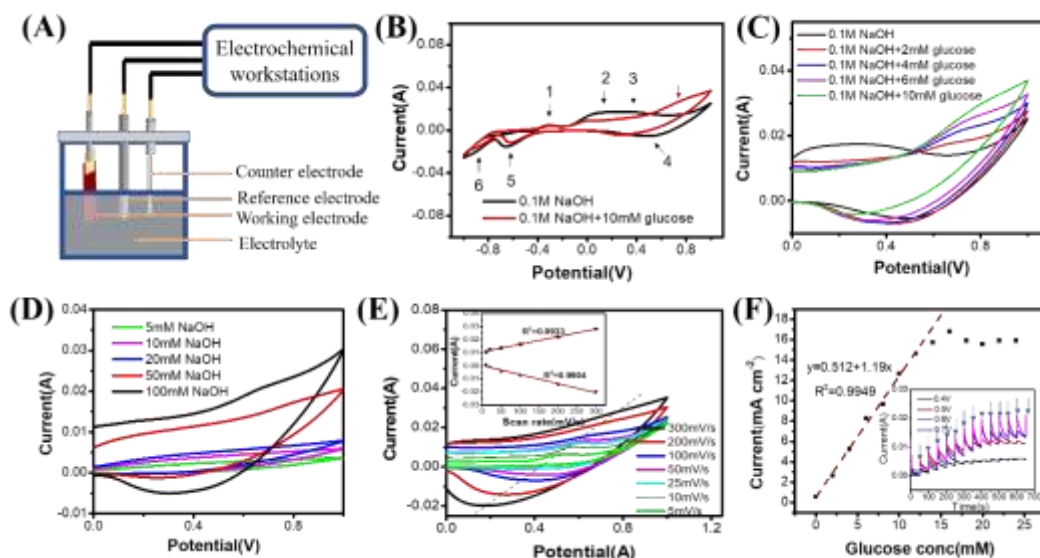


**Fig. S10** (A) Schematic diagram for glucose sensing. Current response versus different conditions using Cu/cellulose papers as the electrode for glucose sensing. (B) CV curves of the conductive paper in the presence and absence of glucose. (C) CVs of the conductive paper in the presence of glucose with different concentrations. (D) CVs of the conductive paper with the appearance of 2 mM glucose under different concentrations of NaOH. (E) CVs of conductive paper at different scan rates. Inset shows plots of peak current as a function of scan rate and linearly fitted curves. (F) Normalized current response versus the concentration of glucose. The insert showed the real time current response of conductive paper at various potentials with successive additions of 2 mM glucose, and the arrows means the steps that we added the certain concentration of glucose.

To illustrate the electrochemical activity of Cu/cellulose paper, we performed measurements using the common example of glucose sensing as illustrated in Figure S10A. The cyclic voltammograms (CVs) of the Cu/cellulose paper electrode in the presence and absence of glucose were showed in Fig. S10B, six well-demarcated reversible redox peaks can be distinctly observed on the paper electrode before the addition of glucose. This is assigned to the well-known electrochemical process involving the multistep reversible transition of Cu(0)/Cu(I), Cu(0)/Cu(II) accompanied by Cu(I)/Cu(II), and Cu(II)/Cu(III) in an alkaline system. In the presence of 2 mM glucose, the broad peak 3 at 0.27 V that is correlated with the generation of Cu(III) species from the Cu(II) solid(s) and hydroxide ions almost disappears and is replaced by a clear shoulder peak at 0.65 V during the anodic scan. The differences can be solely ascribed to the oxidation

of glucose on the Cu paper electrode assisted by the Cu(II)/Cu(III) redox couple.<sup>1</sup> The CV measurements of conductive paper electrode performed at different scan rates were showed in Fig. S10E. The comparative profiles show that the redox peak currents changed linearly and excellent correlation coefficients are determined, indicating the kinetic surface adsorption/diffusion dominant electro-oxidation of glucose on Cu paper. Fig. S10C presents the performance of the sensor under different glucose concentration. As desired, both of anodic shift of the peak potential and dramatic enhancement of the oxidative peak current are observed. However, a cathodic potential shift does not appear and the peak current has only a slightly increase. This indicates a nonreversible electrochemical oxidation process. Besides, owing to the largely formed hydroxyl radical at high applied potential, the anodic current could also increase significantly with the elevating of NaOH concentration (Fig. S10D). We choose 100 mM NaOH as ultimately selected alkaline electrolyte for subsequent tests. Specifically, we performed typical current vs time (i-t) measurements using the Cu/cellulose paper as the working electrode that was biased to various imposed potentials. As shown in the insert in Figure S10F, each addition of glucose to the solution resulted in an increased current with the current being higher for higher imposed potentials. Figure S10F shows the corresponding linear dependence of current response versus glucose concentration for an imposed 0.6 V potential. The sensitivity of the Cu/cellulose paper was determined to be 1190 mA mM<sup>-1</sup> cm<sup>-2</sup>. Furthermore, the limit of detection of Cu/cellulose paper is 4.7 μM, S/N = 3, whereas the liner range of Cu/cellulose paper electrode is 2-12 mM. Thus, the as-prepared Cu/cellulose paper electrode shows relatively high sensitivity, fast response, good high-concentration susceptibility and low detection limit. These benefits may be ascribed to the large surface area and high conductivity conferred by the copper NPs. Therefore, the Cu/cellulose paper may have potential applications in electrochemical applications for sensing or energy conversion.

**Table S1.** Sheet resistance( $R_s$ ) or conductivity of Cu-based electrodes on different substrates.

Electrodes	Methods	$R_s$ or conductivity	References
Cu/PET film	SU-8-Induced solution-process	$20 \times 10^{-3} \Omega/\text{sq}$	2
Cu/PEN film	Bar-coating	$< 1 \Omega/\text{sq}$	3
Commercial Cu foil tape	—	$3.61 \times 10^{-3} \Omega/\text{sq}$	3
Cu/PI film	Polyelectrolyte-induced solution-process	$47.3 \times 10^{-2} \Omega/\text{sq}$	4
Cu/PDMS	Polyelectrolyte-induced solution-process	$1 \times 10^5 \text{ S m}^{-1}$	5
Cu/PET yarn	Polyelectrolyte-induced solution-process	$0.17 \Omega/\text{sq}$	6
Cu/PDMS	Transfer printing	$105.32 \Omega/\text{sq}$	7
Cu/PET	Transfer printing	$115.45 \Omega/\text{sq}$	7
Cu/PET	Spin-coating	$1.62 \times 10^8 \Omega/\text{sq}$	8
Cu/PET	Spin-coating + acetic acid treatment	$42.8 \Omega/\text{sq}$	8
Cu/PET	Spin-coating + laser sintering process	$1 \Omega/\text{sq}$	8
Cu/cotton fabric	Polyelectrolyte-induced solution-process	$1 \text{ S m}^{-1}$	9

**Table S2.** The resistances and conductivity of Cu paper for EMI detecting with different deposition time.

Samples	ELD time (min)	Thickness ( $\mu\text{m}$ )	$R_s$ ( $\Omega/\text{sq}$ )	Conductivity (S/m)
1	10	$166 \pm 3$	$0.07 \pm 0.03$	86058
2	20	$182 \pm 3$	$0.03 \pm 0.02$	183150
3	30	$190 \pm 3$	$0.02 \pm 0.01$	263852
4	60	$194 \pm 3$	$0.01 \pm 0.01$	515463

**Movie S1.** The self-cleaning property of Cu/cellulose paper.

**Movie S2.** The self-cleaning property of Cu/cellulose fabric.

1. Y. X. Zhao, L. L. Fan, Y. Zhang, H. Zhao, X. J. Li, Y. P. Li, L. Wen, Z. F. Yan and Z. Y. Huo, *ACS Appl. Mater. Interfaces*, 2015, **7**, 16802-16812.
2. M. Hu, Q. Guo, T. Zhang, S. Zhou and J. Yang, *ACS Appl. Mater. Interfaces*, 2016, **8**, 4280-4286.
3. J. Kwon, H. Cho, H. Eom, H. Lee, Y. D. Suh, H. Moon, J. Shin, S. Hong and S. H. Ko, *ACS Appl. Mater. Interfaces*, 2016, **8**, 11575-11582.
4. R. S. Guo, Y. Yu, Z. Xie, X. Q. Liu, X. C. Zhou, Y. F. Gao, Z. L. Liu, F. Zhou, Y. Yang and Z. J. Zheng, *Adv. Mater.*, 2013, **25**, 3343-3350.
5. X. L. Wang, H. Hu, Y. D. Shen, X. C. Zhou and Z. J. Zheng, *Adv. Mater.*, 2011, **23**, 3090-3094.
6. Z. Z. Zhao, C. Yan, Z. X. Liu, X. L. Fu, L. M. Peng, Y. F. Hu and Z. J. Zheng, *Adv. Mater.*, 2016, **28**, 10267-10274.
7. J. Kwon, H. Cho, Y. D. Suh, J. Lee, H. Lee, J. Jung, D. Kim, D. Lee, S. Hong and S. H. Ko, *Advanced Materials Technologies*, 2017, **2**, 1600222.
8. Y. Zhang, J. N. Guo, D. Xu, Y. Sun and F. Yan, *Nano Research*, 2018, **11**, 3899-3910.
9. X. Q. Liu, H. X. Chang, Y. Li, W. T. S. Huck and Z. J. Zheng, *ACS Appl. Mater. Interfaces*, 2010, **2**, 529-535.